Evaluation of Self-Compacting Rubberized Concrete Properties: Experimental and Machine Learning Approach

Olatokunbo M. Ofuyatan*
Department of Civil Engineering, College of Engineering,
Covenant University, Ota, Lagos, Nigeria
Email: olatokunbo.ofuyatan@covenantuniversity.edu.ng
http://orcid.org/0000-0001-9052-2758

Imrose B. Muhit
School of Computing, Engineering and Digital Technologies,
Teesside University, Tees Valley TS1 3BX, United Kingdom
Email: i.muhit@tees.ac.uk
https://orcid.org/0000-0002-5263-8925

Adewumi J. Babafemi
Department of Civil Engineering, Faculty of Engineering,
Stellenbosch University, Stellenbosch, South Africa
Email: ajbabafemi@sun.ac.za
https://orcid.org/0000-0002-6232-6642

Ibukunoluwa Osibanjo
Department of Civil Engineering, College of Engineering,
Covenant University, Ota, Lagos, Nigeria
Email: ibukunoluwa.osibanjo@stu.cu.edu.ng

Corresponding Author
Olatokunbo.ofuyatan@covenantuniversity.edu.ng

Journal: Structures, Volume 58, December 2023, 105423

Published Version: https://www.sciencedirect.com/science/article/pii/S2352012423015114

DOI: https://doi.org/10.1016/j.istruc.2023.105423

Full Citation: Ofuyatan, O. M., Muhit, I. B., Babafemi, A. J., & Osibanjo, I. (2023). Evaluation of self-compacting rubberized concrete properties: Experimental and machine learning approach. *Structures*, 58, 105423.

ABSTRACT

Diverse negative impacts of waste tire disposal have created a menace to a cleaner environment worldwide. Global awareness on the use of unconventional materials in concrete necessitated the use of solid waste in concrete. Towards sustainable construction and building materials, in this study, powdered waste rubber tires (PWRT) were incorporated into self-compacting concrete as a partial substitute for fine aggregate. The suitability of the self-compacting rubberized concrete (SCRC) was assessed by conducting workability tests (slump flow, T50, and L-box), mechanical tests (compressive, splitting tensile, and flexural strength tests), microstructural analysis, and durability tests. The results showed that an increasing percentage of PWRT had an adverse effect on the workability and flowability of SCRC. Mechanical strength at 3, 7, 21, 28, 56, and 90 days exhibited a reduction with an increasing PWRT content. Furthermore, the microstructural analysis showed weaker adhesion at the interfacial transition zone in the SCRC. A correlation matrix with empirical relationships was also developed. The effect of acid attack on SCRC was measured by immersion in HCL and Na_2SO_4, and a poor resistance was noticed. Machine learning regression algorithms were employed to predict the SCRC mechanical properties, including linear, ridge, lasso, decision tree, random forest, extreme gradient boosting, and support vector. In addition, evaluation metrics with statistical checks were also used to assess the model's performance. Ridge regression appeared best suited for predicting the compressive strength, while random forest regression best estimates the tensile and flexural strength.

Keywords: self-compacting rubberized concrete, powdered waste rubber tires, mechanical properties, durability tests, machine learning, regression models.

1. INTRODUCTION

A continually changing world requires constantly improving its construction methods. Concrete is one of the most often utilized construction materials in the modern world. This may be due to various factors, including its behavior, strength, affordability, durability, and flexibility, in addition to the wide range of uses it provides. The invention of high-performance self-compacting concrete (SCC) is one of the most significant developments in concrete technology. It is a non-segregating concrete that doesn't require mechanical consolidation to flow, spread, fill forms, and encase reinforcements [1-6]. SCC is mostly utilized to build intricate concrete frames because of its remarkable flowing qualities, and its use guarantees reduced energy consumption, construction, and labor cost [3, 4]. The advent of SCC stands out among other trends and advancements in the building industry as having an acceptable potential and piqued interest in using alternate raw materials, wastes, byproducts, and secondary minerals as mineral additives [5].

Moreover, SCC can efficiently go through crowded reinforcements due to its rapid flow rate, cohesion, and good passing ability, i.e., only the weight of the object allows it to flow freely [6]. Although SCC is frequently utilized in construction works, an appropriate SCC design mix is still challenging. The primary cause is that SCC is a quasi-brittle material with low due to the compact microstructure and low water-cement ratio, the yield strength is unsatisfactory/poor [7]. SCC requires relevant flowability and passing ability, and more often, added industrial wastes might increase the uncertainty related to the flowability and heterogeneity of the concrete itself [8]. It is evident from the literature that industrial wastes and byproducts like fly ash [8, 9], silica fume [8, 10], ground granulated blast furnace slag [8, 11, 12], cow bone [12], and palm ash [13] can be partially replaced for the cement in the cementitious system in a motivation to lower the carbon emissions and reduce the landfill waste.

Every year, thousands of tons of used rubber products like worn tires are abandoned and disposed of improperly, causing serious environmental pollution to our air, water, and land and affecting the health of our terrestrial and aquatic ecosystems. The rising number of trash tires has already become a global issue, and an estimated 5 billion tires are anticipated to be disposed of regularly by 2030 [14]. Although landfilling of tires is the best example of proper handling (while not recycling), landfilling such materials poses a severe environmental danger as waste tire disposal locations, in particular, contribute to biodiversity loss, as these contain hazardous and soluble components [14]. Moreover, burning rubber tires releases greenhouse gases (GHG), including CO_2

and carbon black particles, that are harmful and create enormous environmental pollution [14, 15]. Rubber particles can be utilized and included in cement-based materials as this will mitigate the pollution issues (including the burning of tires) and serve as a recipe for an innovative and cheaper alternative to building materials to reduce the embodied carbon in the construction industry [16]. The prospect of designing self-compacting rubberized concrete (SCRC) is particularly appealing because this new material exhibits the properties of SCC while taking advantage of the inclusion of scrap tire rubber.

There have been a few research [10, 14, 15, 17-23] on self-compacting concrete that uses tire rubber as a substitute for fine and/or coarse natural aggregate at various percentages. When chunk and chipped rubber were utilized as a partial replacement for coarse aggregate, compared to regular concrete, these properties tended to deteriorate and lessen: compressive strength, flexural strength, and modulus of elasticity. Weak bonding between the cement paste and rubber particles at the interfacial transition zone (ITZ) is one reason for the drop in strength [23]. Of course, the lower stiffness of the rubber aggregate compared to natural aggregate is another reason.

Although better results were achieved when replacing fine aggregate instead of coarse aggregate [10], there is not enough literature that underpins the prospect of SCRC when powdered waste rubber tires (PWRT) are utilized as a partial replacement of fine aggregates. This research gap is one of the motivations of the current study. Partial or full replacement of fine aggregates in SCRC has the potential to significantly reduce the consumption of natural sand while paving the way for alternative use of rubber tires. To assess the stability and reliability of SCRC, some properties (e.g., durability performance, dynamic behavior, fracture behavior, impact resistance, etc.) have been studied in addition to compressive strength [22, 24-26]. However, the unconfined compressive strength (UCS) (i.e., maximum axial compressive stress under zero confining stress) received primary attention in determining the strength performance of SCRC.

Global businesses are undergoing a transition in response to the Fifth Industrial Revolution (5IR), and the construction sector or industry cannot be left behind. Soft computing techniques, like machine learning (ML) or artificial neural networks (ANN), are becoming increasingly popular among researchers to model and estimate concrete characteristics. Artificial intelligence solutions are being steadily implemented at all stages of the development process [27, 28]. The compressive strength of SCC with silica fume as an additional cementitious material was calculated and

determined by Azizifar and Babajanzadeh [29] using artificial intelligence techniques like Multivariate Adaptive Regression Splines (MARS) and Gene Expression Programming (GEP) methodologies as reliable methods to predict UCS.

Similar properties were estimated for similar concrete types (i.e., silica fume incorporated SCC) by Serraye et al. [30] using ANN. Kaloop et al. [31] employed the gradient tree boosting machine (GBM) approach and estimated the compressive strength of high-performance concrete. de-Prado-Gil et al. [32] used a collective machine learning model. The UCS of SCC containing recycled aggregates was visualized using (Random Forest, K-Nearest Neighbor, Extremely Randomized Trees, Extreme Gradient Boosting, Gradient Boosting Machine, Category Boosting, and the generalized additive models like Inverse Gaussian and Poisson). Predicting the compressive strength of rubberized concrete using ML algorithms also got some attention from a few researchers in recent years. For instance, Li et al. [33] exercised GEP to establish empirical models for concrete made with NaOH-treated crumb rubber. Algorithms like ANN, fuzzy logic, GEP, k-nearest neighbor, regression trees, random forests, Gaussian process regression, and support vector machine were utilized by researchers [34-39] for rubberized concrete; however, they were limited to only compressive strength modeling. On the contrary, only a few research [40, 41] explored the SCRC modeling and utilized Gaussian process regression, beetle antennae algorithm-search-based random forest, multi-layered perceptron artificial neural network (MLP-ANN), sets of MLP-ANNs and regression tree cluster; nevertheless, limited to UCS prediction only. The fundamental motivation of this study is to address this research gap while further exploring the SCRC field in estimating the additional governing mechanical properties and identifying the optimum prediction performance of ML algorithms.

2. RESEARCH SIGNIFICANCE

This study has been undertaken in a bid to achieve environmental sustainability in solid waste management and environmental pollution control [42] and the development of green concrete, which is in line with the United Nations Sustainable Development Goals 9 (ensure resilient infrastructure), 11 (make cities and human settlements inclusive, secure, and sustainable), and 12 (guarantee sustainable consumption and production patterns) [43]. Hence, an evaluation of the characteristics of SCC by substituting fine aggregate (sand) with PWRT in its fresh and hardened states was conducted, including examining its microstructures. A correlation matrix between

different mechanical properties was further developed. Furthermore, identification, optimization, and testing of ML techniques/algorithms to estimate the mechanical properties (compressive, flexural, and split tensile strength) of SCRC were conducted. Bearing that several hyperparameters still require optimization to achieve their optimum prediction performance, several ML approaches for forecasting the mechanical parameters (compressive, tensile, and flexural strength) of the SCRC using ensemble modeling with Python were analyzed and compared. A decision tree with a bagging technique is utilized, and 25 sub-models are created for optimization to produce a reliable result. To determine the best model, comparisons are done with an individual, ensemble, and gene expression programming. Seven distinct regression methods were employed to predict the strength, including Linear Regression, Ridge, Lasso, Decision Tree Regression, Random Forest Regression, Extreme Gradient Boosting Regression (XGBR), and Support Vector Regression (SVR).

A quick and efficient prediction of the mechanical properties of SCRC significantly reduces the challenges and uncertainties with laboratory-based estimation. It optimizes costs by reducing time costs in traditional computational modeling. This will certainly leverage the digital transformation agenda of the construction industry of many countries [44]. Hence, the scientific novelty of this study is to establish a mixing ratio of SCRC while partially replacing fine aggregates (real physical experimental data) and assessing the efficacy of the ML strategies in predicting similar properties of SCRC.

3. EXPERIMENTAL PROGRAM PERFORMED

3.1 Materials

The material for the investigation includes CEM II 42.5 N (high-quality general-purpose cement), coarse aggregate (granite) 12 mm maximum, and river sand with a fineness modulus of 1.80. In addition, Conplast SP430 superplasticizer, a chloride-free sulphonated naphthalene-based polymer, was used to modify the workability of the mix. The water-to-cement ratio (w/c) was maintained constant for each mixture at 0.45. Waste rubber tire was sourced locally, cleaned, and air-dried; thereafter, the tires were pulverized and sieved (see Figure 1).

Figure 1. Powdered waste rubber tires (PWRT) sample

3.2 Self-Compacting Concrete Mix Design

The mix design proportion used was 1:1:1.5 (cement: fine aggregate: coarse aggregate) at a w/c of 0.45. Table 1 shows the mix proportions of the constituent materials. Mixing the constituent materials was accomplished by hand until a homogenous mixture was achieved. Water and the chemical admixture were added to the dry mix to form a homogenous paste. The superplasticizer dosage was 1.5% of the binder (cement), which is within the recommended limit [45, 46] for high-performance concrete.

After mixing, a workability test using the slump cone was conducted. Test specimens for compressive strength and splitting tensile strength were cast using 150 mm cube and cylindrical molds of 100 mm × 200 mm, respectively (see Figure 2(a)). Test specimens of 100 mm × 100 mm × 600 mm were built to gauge the flexural strength of the SCRC beams.

The molds were lubricated properly with used engine oil beforehand and filled with SCC without vibration. The concrete was mixed in the open air, but the specimens were kept in the laboratory soon after casting. The samples were then removed from the mold after 22±2h and cured by complete immersion in water at room temperature, as shown in Figure 2(b). Samples were tested at 3, 7, 21, 28, 56 and 90 days.

Table 1. SCRC blending proportions

Mixes	Cement (kg)	Sand (kg)	Granite (kg)	Replacement (kg)	Water (kg)
Control	25.00	25.00	37.50	0.00	11.00
PWRT 5%	25.00	23.75	37.50	1.25	11.00

PWRT 10%	25.00	22.50	37.50	2.50	12.00
PWRT 15%	25.00	21.25	37.50	3.75	12.00
PWRT 20%	25.00	20.00	37.50	5.00	12.00

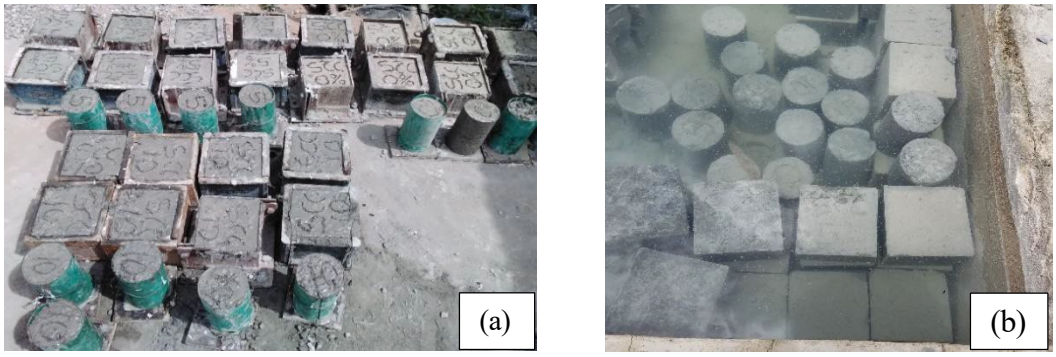

Figure 2. (a) casting (b) curing of the self-compacting rubberized concrete samples

3.3 Fresh Properties

The fresh state properties, slump flow, T_{50}, and L-box testing were performed per the method described in Ofuyatan et al. [1]. The slump flow and T_{50} cm assess the deformability and flowability without hindrances [1, 47]. The result provides information on the filling capacity of SCC. T_{50} cm time obtained is also a gauge for the flow velocity of SCC [48, 49]. The slump value is primarily affected by the w/c and mix ratio. For the V-funnel apparatus, the duration of flow is measured. The L-box test obtained the self-compacting concretes' filling and passing ability, and segregation was investigated by [50, 51].

3.4 Hardened Properties

The compressive strength was assessed following BS EN 206 using 150 mm cubes [52]. The compression-testing machine was used to carry out an ASTM C496-compliant splitting tensile strength test [53]. The test was conducted using a 100 mm × 200 mm cylindrical sample. According to ASTM C78 [54], flexural tests were carried out utilizing beams with third-point loads. The load at which failure occurred for each test was monitored and noted at 3, 7, 21, 28, 56, and 90 days. Scanning electron microscopy (SEM) was also conducted on tested hardened samples to observe the microstructure of SCRC.

3.5 Durability Properties

The durability of concrete can be defined as its capacity to withstand deterioration caused by weathering, abrasion, chemical attack, or other processes. If concrete is deemed durable, it implies

that it has maintained its original shape, quality, and functionality when subjected to operating conditions. Chemical attack is a significant factor that can cause the deterioration of concrete structures by inducing volume changes and cracking, making it a primary concern for concrete durability, among other factors. The durability analysis aims to ascertain and estimate the effect of HCL (hydrochloric acid) and Na_2SO_4 (sodium sulfate, sodium salt form of sulfuric acid) on concrete incorporated with PWRT at different replacement percentages.

3.6 Results and Discussion

3.6.1 Workability Tests (Slump, T_{50}, and L-box Tests)

The diameter and duration of the slump flow (T_{50}) are presented in Figure 3. From the figure, the slump flow diameter decreases as the partial substitution of PWRT increases from 0% to 20%. The maximum slump flow diameter of 680 mm is recorded for SCC containing 5% of PWRT, which is 3% less than the control. At 20% of PWRT, the decrease in the slump flow diameter is 17%. For the T_{50} test, the time to reach the 50 cm mark on the flat board increases as the PWRT content rises from 0% to 20%, as depicted in Figure 3. This is due to the reduction in the flowability of the concrete. The lowest T_{50} time for the mixtures with PWRT is 2.5 sec at 5%. The slump value of the concrete decreased as the quantity of rubber in the mix increased because rubber requires more water. This increase in water demand negatively impacts effective hydration and reduces homogeneity in the mixture. As reported by other researchers, the reduction in the flowability of the SCRC is due to increased frictional resistance of the PWRT and its lower density compared to natural sand [21, 22].

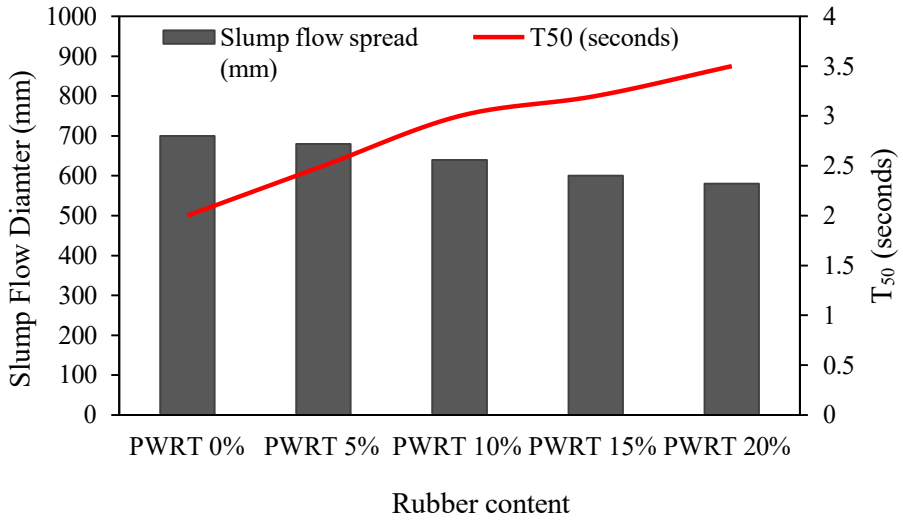

Figure 3. Slump flow and T_{50} for SCRC

L-box tests were performed to assess the influence and impact of PWRT on the flowability of SCC. A high L-box ratio of the fresh flow concrete denotes that the concrete mixture is more fluid (i.e., the mixture has low viscosity) and can flow into narrow and complex spaces (e.g., narrow spaces due to reinforcements) with minimal vibration. From Figure 4, it can be seen that SCC with PWRT has a lower blocking ratio than the control mixture. The lowest blocking ratio for the mixtures with partial replacement of PWRT is 0.51 at 20%, which is approximately 46% lower than the control mix with 0% PWRT.

The drop in workability can be attributable to the higher water absorption of PWRT mixes compared to the control. The water absorption is lower at the 0% mixes, with a 28%, 40%, 45%, and 59% increase in other mixes, which increased the water demand of the mixture and resulted in reduced workability. The water absorption rate of the rubber aggregate used affects its ability to flow and fill voids. A higher absorption rate can reduce the filling ability of the concrete and negatively affect its self-compacting properties. On the other hand, the filling and flow characteristics of the SCC can be enhanced by a low absorption rate in the fine aggregate. Therefore, using fine aggregate is fundamental in the design of SCC made with low absorption rates. Further, a low absorption rate in the fine aggregate can improve the filling and flow properties of the SCC.

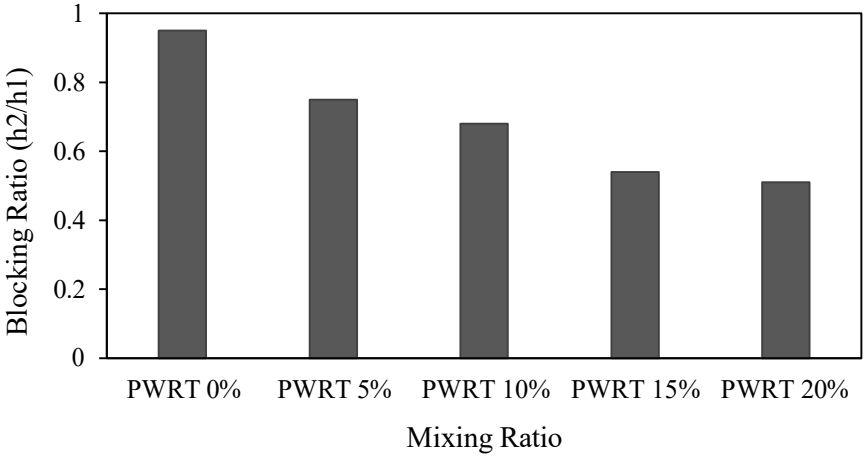

Figure 4. L-box test results of the SCRC

3.6.2 Compressive Strength

Figure 5 compares SCC with and without PWRT to show the impact of PWRT on the compressive strength of SCC. In total, 90 samples were examined at various curing ages, and the findings are

the average of the three tested samples. Generally, when the replacement content rises from 0% to 20%, the compressive strength of the SCRC samples falls. However, as expected, the strength grows with age due to the rate of hydration. At a replacement content of 5% after 28 days, SCRC reaches its ideal compressive strength. The reduction in the compressive strength at 28 days, relative to the control, is 12.7%, 28.6%, 48.2%, and 53.2% at 5%, 10%, 15%, and 20% PWRT, respectively. Reduction in strength with PWRT is also observed at 56 and 90 days. A similar trend is reported by Steyn et al. [55], Flores-Medina et al. [56], and Ling [57] with silica fume and plastic waste [58]. The loss in strength can be attributed to the low elastic modulus of the PWRT, the poor bonding of the cement matrix with the PWRT, air trapped on the PWRT surface due to its roughness, and the porosity of SCRC mixes. Additionally, because the rubber aggregate is hydrophobic, the ITZ between the rubber and cement paste is less dense than the link between sand and cement paste [55, 59, 60].

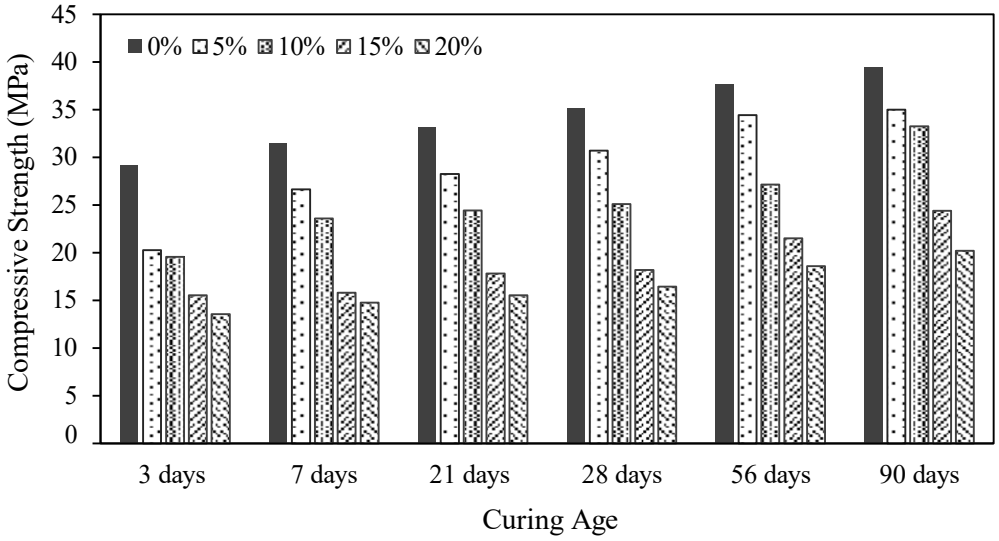

Figure 5. Compressive strength test results of the SCRC

3.6.3 Splitting Tensile Strength

The outcome of the result in the splitting tensile strength is presented in Figure 6. Similar to the compressive strength performance, the splitting strength decreases as the content of the PWRT increases from 0% to 20% but increases with age due to cement hydration. While optimum strength is also achieved at 5% PWRT content as with the compressive strength, the strength reduction in 28 days compared to the control is significant (39.6%). A decrease of 31.6%, 38.8%, 49.7%, and 55.1% is observed at 5%, 10%, 15%, and 20% PWRT, respectively, at 90 days

compared to the control. The reasons for the reduction in the splitting strength are the same as those mentioned for the compressive strength.

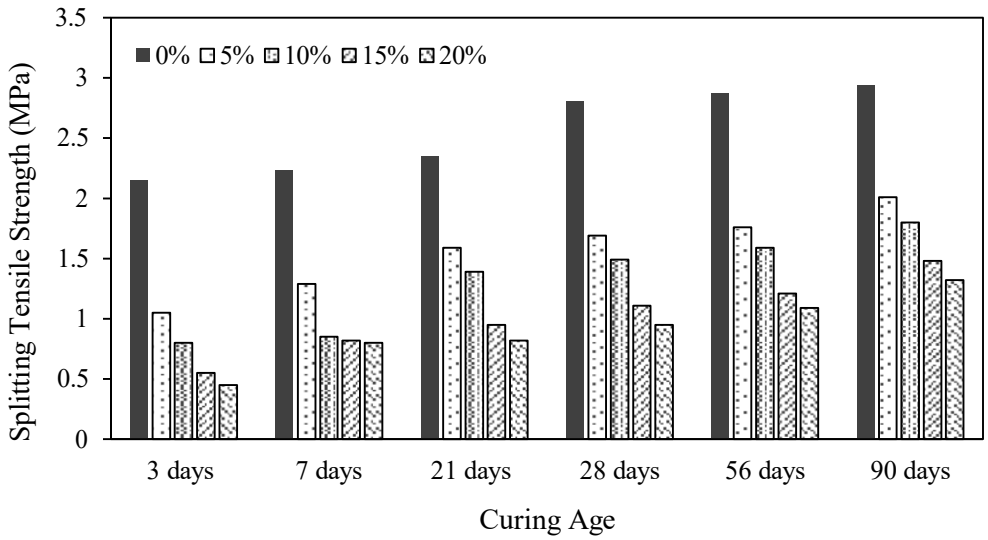

Figure 6. Splitting tensile strength test results of the SCRC

3.6.4 Flexural Strength

The presence of PWRT had a negative impact on the flexural strength of the SCRC beams, much like it did on compressive and splitting tensile strength (see Figure 7). While the strength loss for 5% PWRT compared to control is significant (16.5%) for 3 days, it becomes less noticeable with age. For instance, at 90 days, flexural strength drops by a little over 2% compared to the control specimen. Therefore, SCC with 5% PWRT can be used when high-strength concrete is not required and waste minimization (tire rubber) has priority.

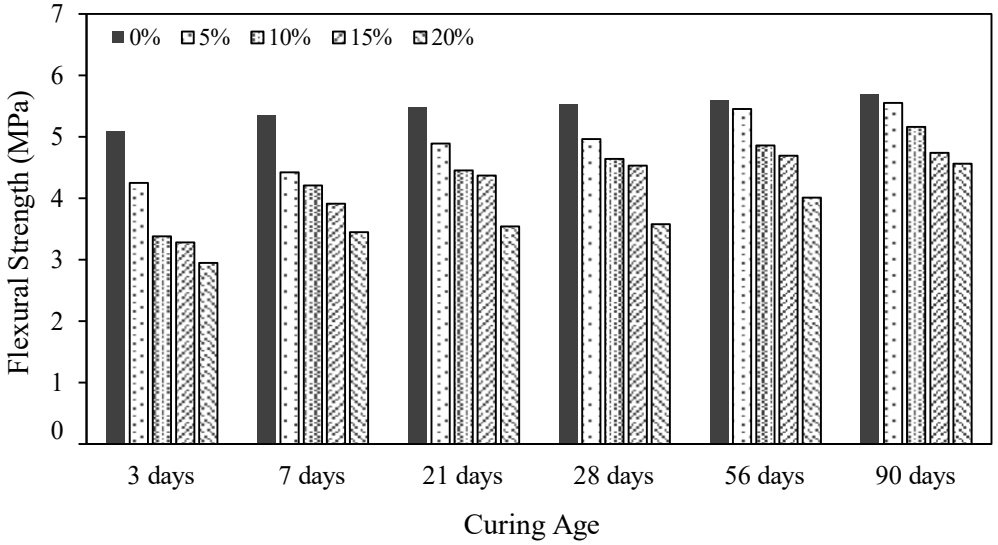

Figure 7. Flexural strength test results of the SCRC

3.6.5 Correlation Matrix

As a statistical indicator, the correlation coefficient measures how linearly related two variables are. This study analyzed the relationship between various mechanical properties using a Python heat map plot in Figure 8. With a correlation coefficient of 0.93, the findings indicated a significant positive association between compressive strength and tensile strength (a coefficient of 1 indicates a perfect positive correlation, i.e., a direct relationship). The association between compressive strength and flexural strength was also quite favorable, with a value of 0.93. With a value of 0.91, tensile and flexural strength showed the least association.

A linear regression analysis was conducted to examine the connections and relationship between these mechanical properties so that if one parameter (say compressive strength) is known, analytically splitting tensile and flexural strength can be determined. The results of the analysis are displayed in Figure 9.

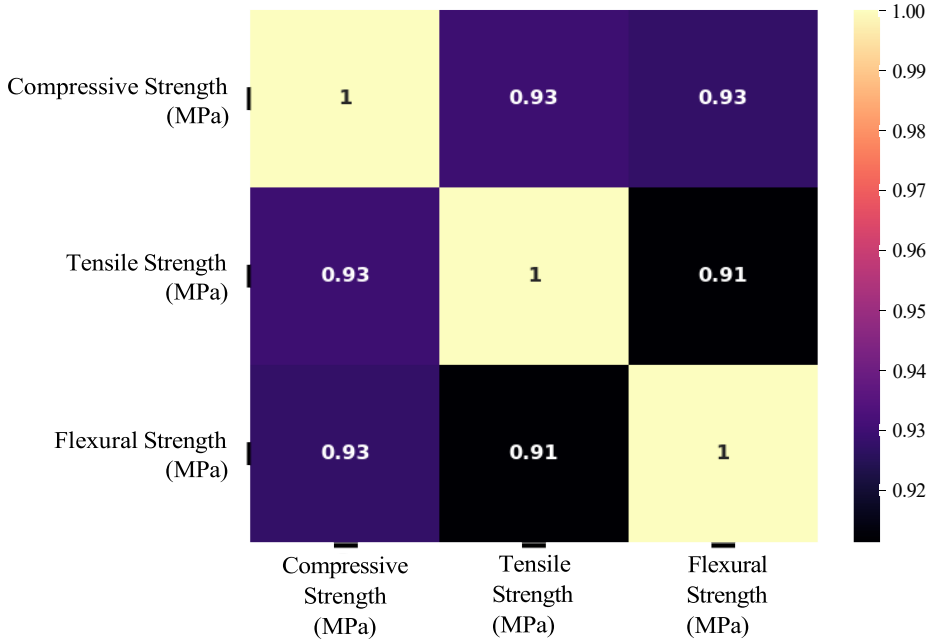

Figure 8. Correlation matrix between the mechanical properties of the SCRC

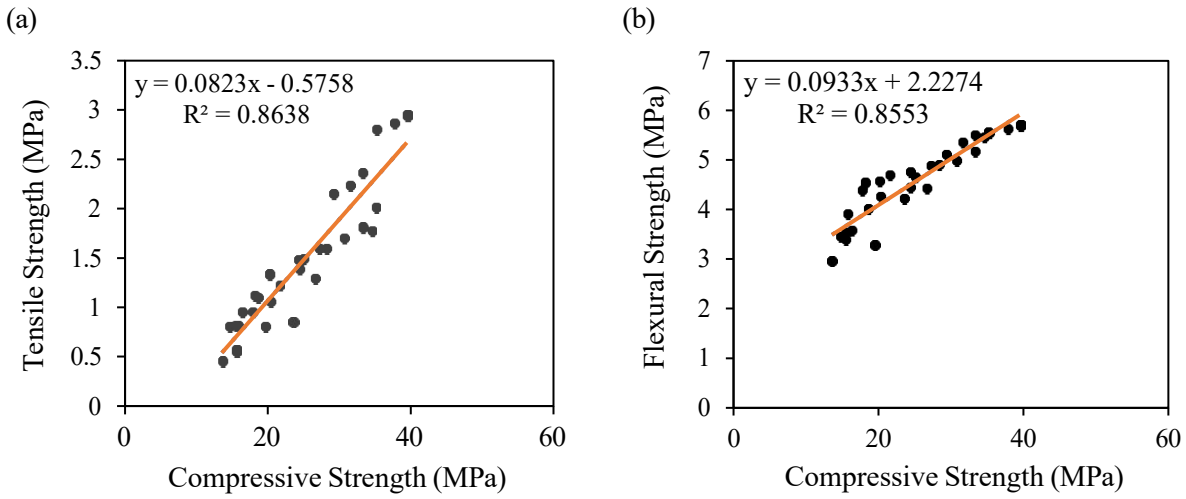

Figure 9. Linear correlation between (a) compressive and tensile strengths and (b) compressive and flexural strengths

As observed, a direct relationship was established between compressive strength and other mechanical properties (i.e., tensile and flexural strengths). The R^2, a measure of the accuracy of the experimental results and validity of the analysis, was determined to be above 0.85 between compressive strength and other mechanical properties. It is worth noting that an increased number of samples (i.e., Monte-Carlo experimental investigations) may further refine these empirical relationships. Hence, the following two empirical equations are proposed to estimate the tensile and flexural strength from compressive strength:

$$f_t = 0.0823 f_c - 0.5758 \quad (1)$$

$$\sigma = 0.0933 f_c + 2.2274 \quad (2)$$

where f_c, f_t, and σ are compressive, tensile, and flexural strengths, respectively.

It is important to appreciate that the proposed linear regression models should only be used to estimate mechanical property levels for which their compressive strength is in the range of the data used to generate the regression equations. Hence, for the clarity of the user, the ranges for the mechanical properties produced in this experiment are tabulated in Table 2.

The utilization of correlation analysis in examining the mechanical characteristics of concrete holds significant value in the optimization of materials, assurance of quality, prediction of structural performance, and advancement of civil engineering. The aforementioned factor assumes

a pivotal position in attaining construction projects characterized by safety, longevity, and cost efficiency, concurrently facilitating advancements in research and development within the field.

Table 2. Statistical parameters for the range of mechanical properties

Properties	Minimum (MPa)	Maximum (MPa)	Mean (MPa)	Std. Deviation
Compressive strength	13.56	39.45	24.91	7.68
Tensile strength	0.45	2.94	1.47	0.68
Flexural strength	2.95	5.68	4.55	0.78

3.6.6 Microstructural Analysis of the SCRC

SEM examines the sample bond structure on a micro-scale. From Figure 10a, the smooth outlook of the control sample suggests excellent interfacial adhesion between the components of the concrete. As the amount of PWRT increases in the SCRC (see Figures 10(b) to 10(e)), sharp outlines and darker patches become visible on the SCRC, suggesting weaker adhesion at the ITZ. The presence of larger micro-clusters (lumps) and deep voids after curing is attributed to the cause of the decreased hardened properties of SCRC with increasing PWRT.

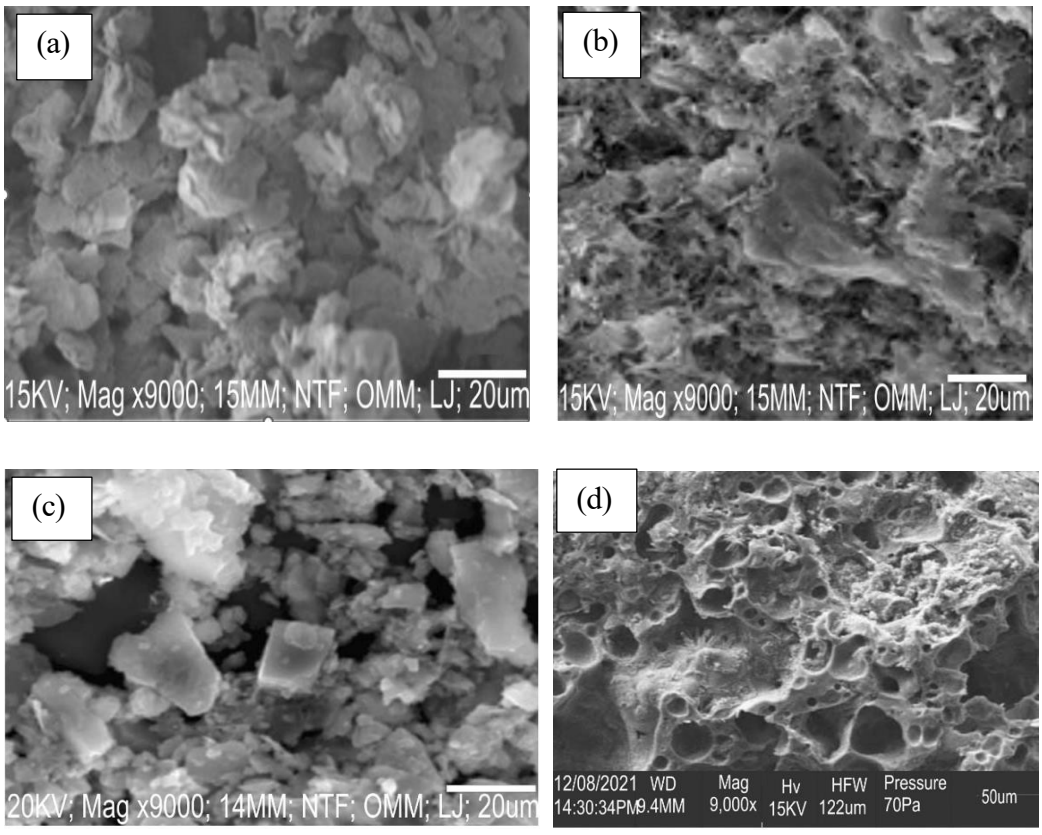

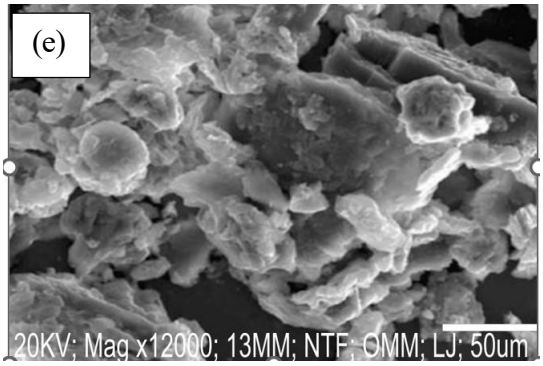

Figure 10. SEM micrograph (a) control sample (PWRT 0%), (b) PWRT 5% sample, (c) PWRT 10% sample, (d) PWRT 15% sample, (e) PWRT 20% sample

3.6.7 Durability of SCRC

Figure 11 presents the results of the acid attack on the 28-day compressive strength of SCRC cured by immersion in HCL and Na_2SO_4. The control mix (PWRT 0%), after being immersed in HCL and Na_2SO_4, has a compressive strength of 12.7 MPa and 13.3 MPa, respectively. There is a clear decrease in the compressive strength when PWRT contents increase, as shown in Figure 11(a). The percentage change in compressive strength (relative to the control specimen) for HCL and Na_2SO_4 is marginally similar for all SCRC samples. The highest (79%) change in compressive strength is observed for 20% PWRT under HCL.

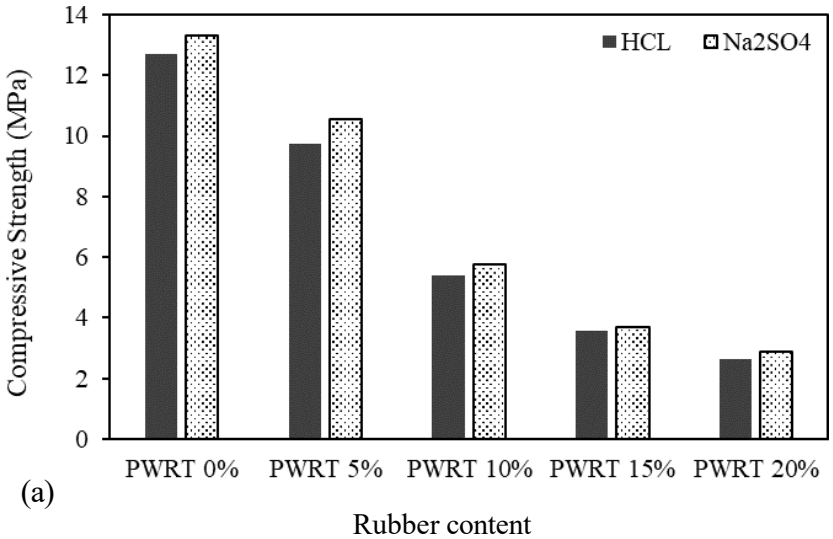

(a)

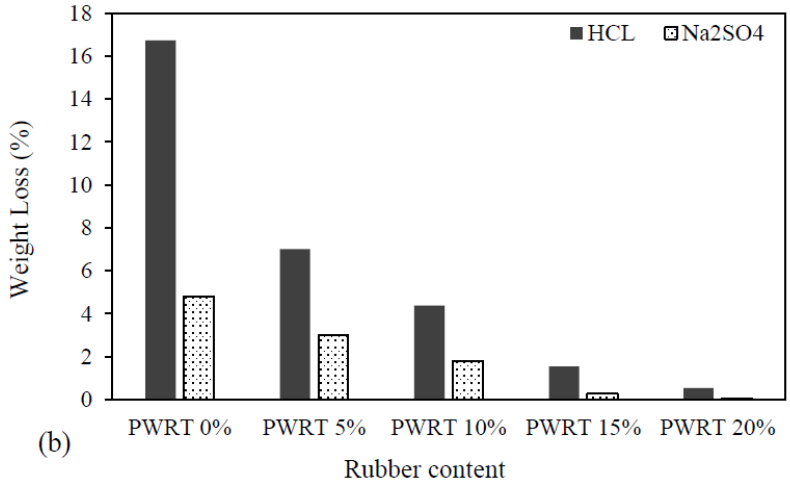

Figure 11. (a) Compressive strength and (b) weight loss after immersion in HCL and Na_2SO_4

Additionally, the weight of all SCRC mixes decreased upon exposure to the chemicals, as indicated in Figure 11(b). The weight reduction (%) can be attributable to the substantial amounts of synthetic polymer in the PWRT and Portland cement's CaO and $Ca(OH)_2$ hydration product, which is mainly responsible for the SCC's weak resistance to acidic attack [61, 62].

4. MACHINE LEARNING APPROACH

Machine learning (ML) methods have become a popular tool for analyzing large volumes of data systematically and efficiently. They have been found to produce rapid and more precise outcomes, thereby diminishing error rates to insignificant levels. These methods are especially useful in tasks involving data of high dimensionality, for instance, regression, classification and clustering. ML can facilitate the generation of dependable and consistent decisions by assimilating past computations and identifying patterns from vast databases. Supervised, unsupervised, and reinforcement learning are the three main classifications of ML. In this study, mechanical parameters of SCRC with varying rubber content, including strength in compression, tensile strain, and flexural strain, were predicted using supervised ML regression models. By using labeled examples during the training phase, the supervised learning algorithm acquires the ability to effectively map input data to output data. It is crucial to enable ML algorithms to draw accurate conclusions from new data, providing them with a substantial amount of data and the expected conclusions. When presented with new data, sufficient training data enables the algorithm to learn and derive the right conclusions [62].

Figure 12 shows a schematic illustration of supervised learning. The training set for the datasets consisted of the first 25 observations, and the test set consisted of the final 5 observations. Python was used to program all regression techniques and calculations.

4.1 Preprocessing

In the present study, the datasets under analysis, according to the Shapiro-Wilk normality test results [63], the data were discovered to be normally distributed. This test is deemed more appropriate for small sample sizes comprising less than 50 samples. If the related p-value in the Shapiro-Wilk test exceeds the significance level, which is typically 0.05, and if the null hypothesis is not confirmed, it is concluded that the data is normally distributed. If the p-value is below or equivalent to the threshold for significance level, the null hypothesis is rejected, and it is concluded that the data are not significant. For compressive, tensile, and flexural strength, the p-value was calculated as 0.125, 0.074, and 0.214, respectively. Normalization is a crucial preprocessing step in ML, particularly when dealing with datasets where variables have varying intervals of variation. When the mean and variance of variables significantly differ, larger mean and variance variables can influence other variables, causing the exclusion of important variables with low variation intervals, ultimately affecting the success of ML models. Therefore, numerical data normalization techniques are utilized to standardize the impact of each variable on the outcome of the regression models. Numerous normalization methods have been developed for normalizing datasets, such as min-max scaling, Z-score normalization, log transformation, and unit vector scaling. This study used the Min Max Scaler method to normalize the data. By dividing the data by the range and subtracting the minimum value from the data (maximum value - minimum value), this technique scales the data to a specified range, often between 0 and 1.

$$x_{scaled} = \frac{x - x_{min}}{x_{max} - x_{min}} \tag{3}$$

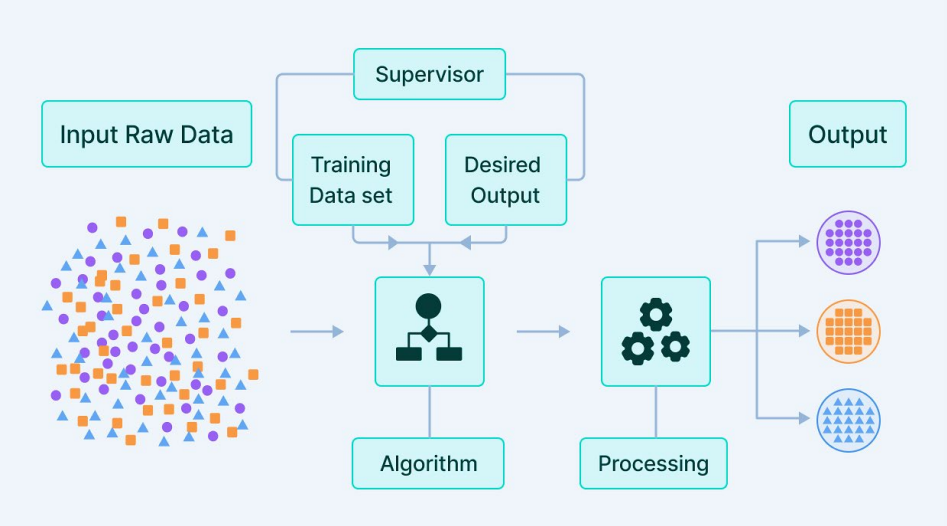

Figure 12. Schematic of supervised learning process (source: Big Data Made Simple)

4.2 Models and Methodologies

The regression technique in ML is utilized to approximate the output value based on the input samples of a given dataset. The fundamental objective of the regression method is to reduce the disparity between the predicted output values and their factual equivalents. This study used seven distinct regression methods, including linear regression, ridge, lasso, decision tree, random forest, extreme gradient boosting regression (XGBR), and support vector regression, to model the flexural, tensile, and compressive strength characteristics of the mixture. The strength in compression, bending strength, and flexural stiffness are SCRC's mechanical properties that were regarded as the dependent variables while curing days and the percentage replacement of rubber were considered independent variables. During the prediction, one of the mechanical properties was chosen as the dependent variable, whereas the remaining ones acted as prediction factors. It is worth noting that, to improve the prediction performance, the maximum deflection obtained from the flexural strength tests was also considered an independent variable to train the models.

4.2.1 Linear Regression

A statistical analysis technique known as linear regression was utilized to determine the relationship between the dependent variable (i.e., output or response) and the independent variable (the input or expected result). By determining the values of the independent variable, the linear regression model calculates the value of the dependent variable. Additionally, there are two distinct categories of linear regression models: simple linear regression and multivariate linear regression [64]. Multiple linear regression relates the relationship between a dependent variable

and two or more independent variables. The key principle underlining the linear regression model is the assumption that a direct correlation exists between the independent and dependent variables. Discussing the multiple variations, in this case, the linear regression model can be represented by the equation:

$$Y = \beta 0 + \beta_1 X_1 + \beta_2 X_2 + \beta_3 X_3 + \ldots + \beta_n X_n + e \quad (4)$$

where Y is the dependent variable's expected value, $\beta 0$ is the intercept, β_1 is the coefficient of the first independent variable (X_1)... β_n is the coefficient of the ultimate independent variable, $\beta_n X_n$, and e is the model error (i.e., degree of variations in the estimation of Y).

4.2.2 Ridge Regression

A method of linear regression is ridge regression used in dealing with the problem of multicollinearity. When two or more independent variables have a high degree of correlation, a phenomenon known as multicollinearity occurs. This makes it difficult to identify the specific impacts of each independent variable on the dependent variable. Ridge regression addresses the problem by introducing an independent term to the regression equation, which helps to reduce the impact of multicollinearity on the model [61]. Ridge regression's method modifies the regression equation by including an independent factor that limits the magnitude of the independent variable coefficients. The penalty term is a function of the sum of the squared values of the coefficients, and it is multiplied by a tuning parameter, λ (lambda), that controls the strength of the penalty. The tuning parameter λ is usually chosen by running a grid search to obtain the optimum lambda value. In the Ridge regression, the regression equation (Equation 4) also includes a penalty term, which is added to the sum of squared errors in the least squares regression equation, $\Sigma (y_i - \hat{y}_i)^2 + \lambda \Sigma \beta_i^2$, where y_i is the actual value, $\hat{y}_i$ is the predicted value, and β_i is the coefficient. By adjusting the value of λ, the degree of shrinkage of the regression coefficients can be controlled to make better predictions.

4.2.3 Lasso Regression

Lasso regression type of regression analysis is referred to as L1 regularization. It is a linear regression method that adds a penalty term to the model to prevent overfitting. Overfitting is a phenomenon in ML where a model adheres excessively to the training data, resulting in poor efficiency when presented with new data. In Lasso regression, the penalty term is the absolute sum of the coefficient times a hyperparameter α, which establishes the degree of regularization. The goal of the algorithm is to minimize:

$$\Sigma (y_i - (\beta_0 + \beta_1 X_1 + \beta_2 X_2 + \ldots + \beta_n X_n))^2 + \alpha \Sigma|\beta_i| \quad (5)$$

Lasso regression has an advantage over ridge regression as it can execute feature selection by identifying significant features and assigning the coefficients of less important ones to zero. This attribute results in simpler and more interpretable models less prone to overfitting [62]. In this study, Lasso's alpha was set at 0.01.

4.2.4 Decision Tree Regression

A decision tree regression model is useful in constructing a model resembling a model tree, where the decisions are represented as branches that split into various potential outcomes. In decision tree regression, each internal node indicates a unique evaluation of an input feature, with each branch representing the corresponding test outcome and each leaf node the prediction (see Figure 13). The algorithm, at every node within the tree, strategically chooses the most optimal feature that splits the data into subsets, displaying the greatest degree of homogeneity with respect to the target variable. By carefully adjusting several hyperparameters, Decision Tree performance can be optimized.

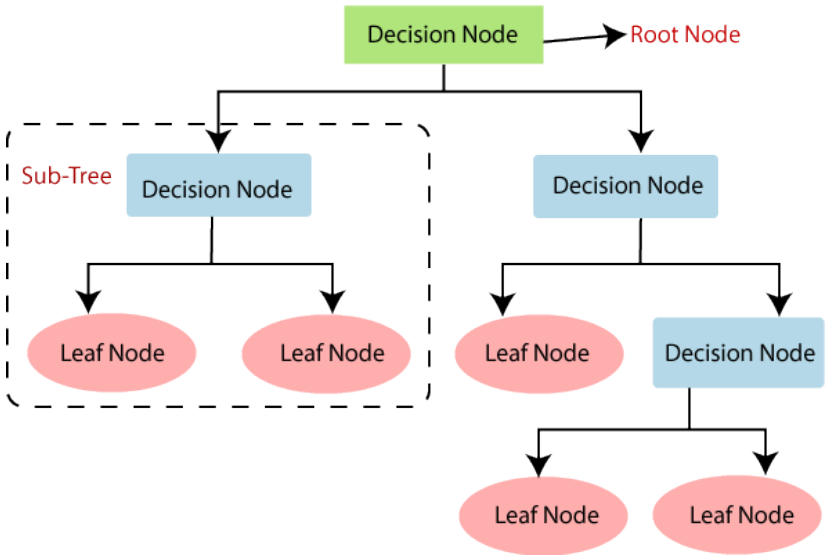

Figure 13. The general structure of a decision tree (source: Google Images)

A few of them are Min_samples_split (which establishes the minimal number of samples necessary to split an internal node), Max_depth (which establishes the maximum depth of the decision tree), Min_samples_leaf is the criterion utilized to specify the minimum number of samples that must be present at a leaf node to determine the quality of a split. The highest number of functions to consider while splitting a node is called max_features. One of the main drawbacks is that it can

easily overfit the training data, especially in instances where the depth of the tree is excessively increased or where too many features exist. Ensemble methods, such as bagging, boosting, and random forests, combine multiple decision trees to reduce overfitting and enhance prediction reliability. In this study, a decision tree was created with the following hyperparameters using a grid search: criterion = ['squared_error', 'absolute_error'], max_depth = [2, 4, 6, 8, 10], min_samples_split = [2, 4, 6, 8, 10], min_samples_leaf = [1, 2, 3, 4, 5], max_features = ['sqrt', 'log2'].

4.2.5 Random Forest Regression

The concept of decision trees and bagging are utilized in the significant ML technique known as random forest regression to generate a highly accurate predictive model. This technique generates a huge number of decision trees by employing a subset selected at random from the input data and a randomly selected subset of the training data. The most accurate prediction [63] is obtained by averaging each individual tree (see Figure 14). This approach enhances the model's accuracy while reducing overfitting. The capacity of Random Forest Regression to handle both linear and nonlinear correlations between the dependent and independent variables is one of its key features. Additionally, it does a good job of resolving missing data and outliers.

In the present study, the random forest was developed with the following hyperparameters: n_estimators, or the number of trees= [10, 50, 100], max_depth = [2, 4, 6], min_samples_split = [2, 4, 6], min_samples_leaf = [1, 2, 4].

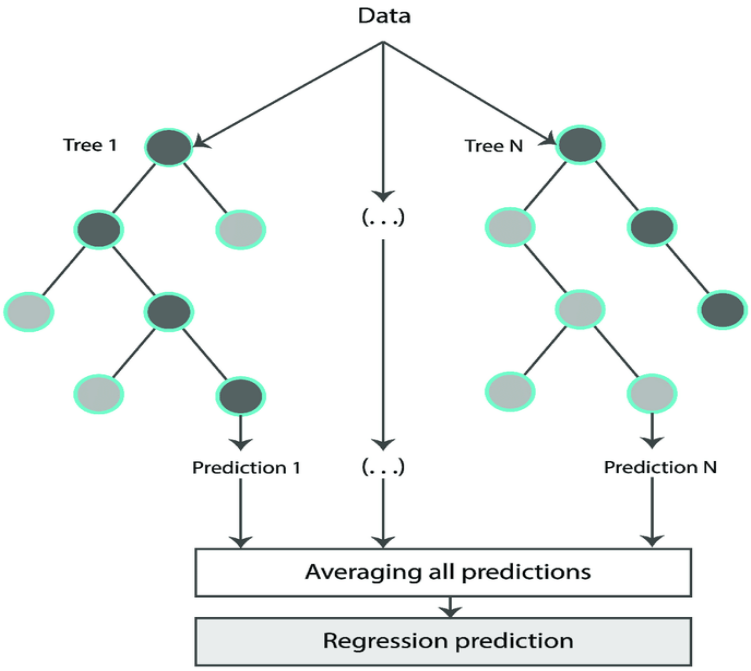

Figure 14. Typical representation of a random forest regressor [64]

4.2.6 Extreme Gradient Boosting Regression (XGBR)

XGBR is a variant of gradient boosting that employs a model parameterization that is more strongly regularized, thereby enabling it to address the problem of over-fitting effectively. It adopts an ensemble prediction approach, leveraging a collection of decision trees. The methodology of XGBR involves an iterative process wherein new decision trees are added to the model to rectify errors made by previous iterations. The approach analyzes errors generated by the previous model on each iteration before fitting an entirely new selection tree to its residuals. One of its significant characteristics is utilizing a gradient-based optimization technique by XGBR to boost model performance. In this study, XGBR was developed using the hyperparameters, estimators = [50, 100, 200], max_depth = [2, 4, 6], and learning rate = [0.1, 0.01, 0.001].

4.2.7 Support Vector Regression (SVR)

The family of support vector machines (SVM), noted for their proficiency in high-dimensional spaces, includes support vector regression (SVR). The fundamental concept of SVR, like SVM, is locating a hyperplane that splits the data into two classes. However, instead of classifying data into discrete categories, SVR is used for continuous prediction. The purpose of SVR is to identify a hyperplane that exists in a space with a large number of dimensions and is positioned as far away from the data points as possible. The hyperplane is selected to minimize the difference between

the anticipated and actual outcome. The objective is to optimize the margin, which is the distance between the hyperplane and the nearest data points. Hyperparameters, including the Kernel function and C parameter, can be tuned to optimize its performance. The decision boundary's shape is determined by the kernel function selected. Common choices include sigmoid linear, radial basis function (RBF) and polynomial. The trade-off between increasing the margin and decreasing the mistake is controlled by the C parameter. In this study, kernel = ['linear'] and C = [1, 10, 100] is used.

4.3 Evaluation Metrics

Five metrics, including the mean absolute error (MAE), coefficient of determination (R^2), root mean squared error (RMSE), mean absolute percentage error (MAPE), and residual sum of squares (RSS), were used to assess the performance and identify the best ML regression models for predicting the mechanical strength parameters. The R^2 number is the most appropriate of the five measures for assessing the accuracy of the models. The percentage of variance in the dependent parameter (mechanical properties) is explained by the uncorrelated variable (model prediction) and is seen to be reflected in the R^2 score. A score of 0.60 to 0.75 is deemed adequate, and a score of 0.75 to 0.95 is deemed superior. Scores above 0.95 are considered good, while those below 0.60 are considered unsatisfactory. However, other evaluation metrics are also applied to boost model confidence. RMSE helps to understand the average prediction error, with lower values indicating better accuracy. RSS measured how closely the model's predictions matched the real data, with lower values meaning better performance. MAPE is useful for assessing percentage differences in predictions, especially when working with different-sized data. Lastly, MAE has the potential to reveal the average size of prediction errors, regardless of direction. Together, these metrics offered a comprehensive assessment of the models' ability to predict the dependent variable effectively, strengthening the rigor of the evaluation.

4.4 Results and Discussion / Observations

4.4.1 Compressive Strength

The models were trained with curing days, percentage rubber replacement, tensile strength, flexural strength, and maximum deflection as independent variables in predicting compressive strength. Table 3 shows the outcome of the evaluation analysis of different ML models used in the study in predicting compressive strength.

Table 3. Performance metrics of different ML models (compressive strength prediction)

ML Models	MAE	R^2	RMSE	MAPE	RSS
Linear Regression	0.079	0.898	0.087	18.120	0.038
Ridge Regression	0.066	0.927	0.074	14.704	0.027
Lasso Regression	0.141	0.625	0.168	19.117	0.140
Decision Tree	0.128	0.706	0.148	32.081	0.110
Random Forest	0.094	0.858	0.103	17.164	0.053
XGBR	0.082	0.870	0.099	19.781	0.049
SVR	0.063	0.923	0.076	15.537	0.029

As indicated in Table 3, ridge regression is considered as the most effective model, achieving an R^2 score of 0.927. A line graph illustrating the actual (experimental) values and the extent to which the predicted values approximate them through ridge regression is shown in Figure 15. It is quite evident that the predicted values are well within the range of true compressive strength values.

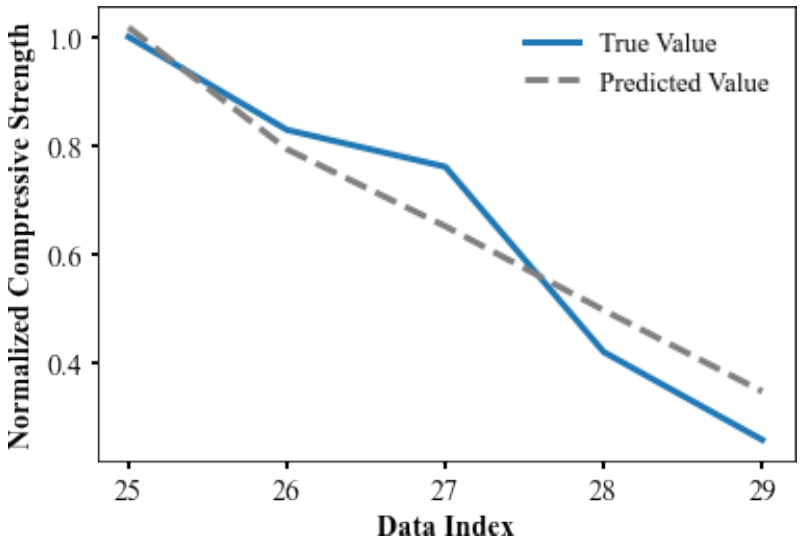

Figure 15. Comparing real data (experimental) and estimated values for compressive strength

4.4.2 Tensile Strength

The models were trained with curing days, rubber replacement, compressive strength, flexural strength, and maximum deflection as the independent variables to predict tensile strength. Table 4 summarizes the outcome of the evaluation analysis of different ML models.

Table 4. Performance metrics of different ML models (tensile strength prediction)

ML Models	MAE	R^2	RMSE	MAPE	RSS

Linear Regression	0.092	0.772	0.109	14.669	0.059
Ridge Regression	0.087	0.795	0.103	13.906	0.053
Lasso Regression	0.079	0.785	0.106	11.976	0.056
Decision Tree	0.119	0.488	0.163	21.442	0.133
Random Forest	0.053	0.933	0.059	10.053	0.018
XGBR	0.062	0.866	0.083	11.734	0.035
SVR	0.114	0.684	0.128	21.045	0.082

This analysis indicates that random forest regression is the most effective model, achieving an R^2 score of 0.933. The best parameters were: {'max_depth': 4, 'min_samples_leaf': 1, 'min_samples_split': 2, 'n_estimators': 50} with the best score of 0.882. Figure 16 illustrates a line graph displaying the actual values and how well the predicted values match them.

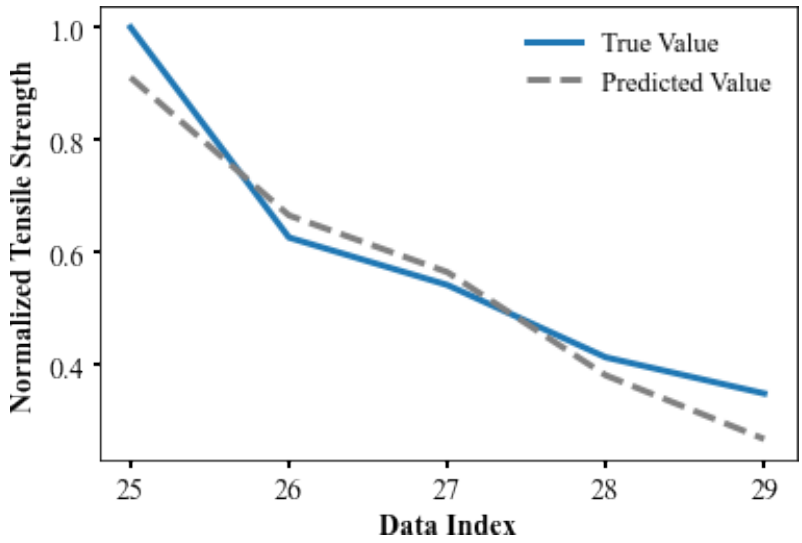

Figure 16. Comparing real data (experimental) and estimated values for tensile strength

4.4.3 Flexural Strength

In a similar approach, the models were trained with curing days, rubber replacement, compressive strength, tensile strength, and maximum deflection as the independent variables to predict flexural strength. The outcome and performance of the ML models are shown in Table 5.

Table 5. Performance metrics of different ML models (flexural strength prediction)

ML Models	MAE	R^2	RMSE	MAPE	RSS
Linear Regression	0.094	0.377	0.127	10.846	0.080
Ridge Regression	0.076	0.585	0.103	8.949	0.053

Lasso Regression	0.094	0.569	0.105	12.689	0.055
Decision Tree	0.059	0.803	0.071	7.877	0.025
Random Forest	0.046	0.889	0.053	5.779	0.014
XGBR	0.048	0.863	0.059	6.200	0.018
SVR	0.063	0.714	0.086	7.433	0.037

As indicated in Table 5, random forest regression outperforms other ML models, achieving an R^2 score of 0.889. The Best Parameters were: {'max_depth': 4, 'min_samples_leaf': 1, 'min_samples_split': 2, 'n_estimators': 10} with the best score of 0.79. Figure 17 shows a comparison between predicted values and true values and how well the prediction model estimates.

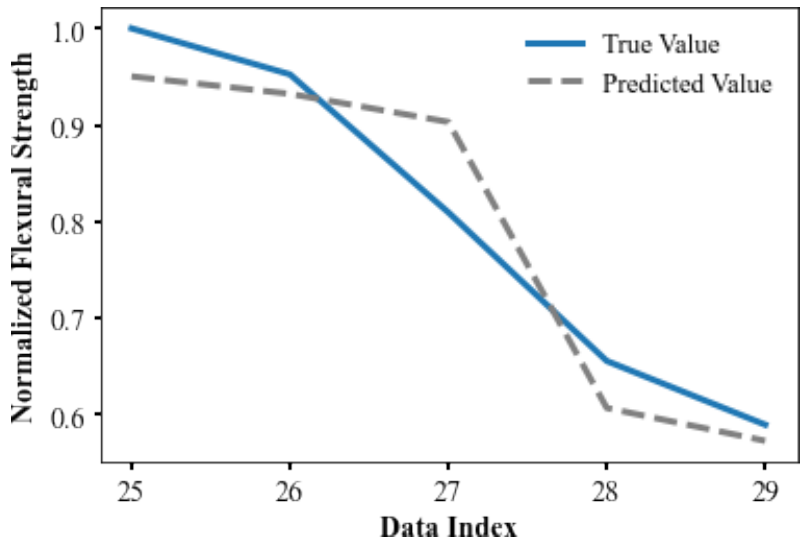

Figure 17. Comparing real data (experimental) and estimated values for flexural strength

In the evaluation of machine learning models, a comprehensive suite of performance metrics was employed to assess their efficacy. Foremost among these metrics was the utilization of R-squared (R^2), a widely accepted measure in regression analysis, chosen for its capacity to elucidate the degree of fit between the model and the observed data, thereby quantifying the proportion of variance in the dependent variable attributed to independent variables. The results obtained suggest that none of the R^2 values exceeded 0.95 across all strength scenarios. However, it is noteworthy that these R^2 values can be deemed statistically robust within the context in which they were applied. Furthermore, in recognition of the potential limitations of R^2 in providing a holistic assessment, further four supplementary metrics were incorporated: Root Mean Squared Error

(RMSE), Residual Sum of Squares (RSS), Mean Absolute Percentage Error (MAPE), and Mean Absolute Error (MAE).

5. CONCLUSIONS

In the experimental investigation, powdered waste rubber tires were incorporated into the self-compacting concrete as a partial replacement of fine aggregates (sand in this case) to reduce the landfill of disposed tires. The powdered tires were used as 5%, 10%, 15%, and 20% replacement of fine aggregates. Workability, flowability, mechanical strength properties (compressive, tensile, and flexural strengths), durability, and microstructural analysis were accomplished. Based on the test results of compressive, tensile, and flexural strength properties, a correlation matrix is developed to identify the linear relationship between these properties. Additionally, the mechanical properties of the self-compacting rubberized concrete were predicted using supervised machine-learning regression models developed using experimental data.

The key findings and outcomes of the study are as follows:

1. The workability and flowability of the self-compacting concrete are reduced when fine aggregates are partially replaced by powdered waste rubber tires (PWRT). An approximate 17% and 46% reduction in slump flow and flowability were observed when incorporated with 20% PWRT.
2. The rise in water absorption is likely responsible for reducing the workability of PWRT mixes compared to that of the control. The water absorption was lower at the 0% mixes, with a 28%, 40%, 45%, and 59% increase in other mixes, which increased the water demand of the mixture and resulted in reduced workability.
3. All SCRC samples experienced a decreased performance in mechanical properties (i.e., compressive, tensile, and flexural strengths) at all curing ages tested. However, at the higher curing ages (90 days), the differences between the control and 5% PWRT mix are insignificant except for tensile strength. Depending on the design requirement, 5% PWRT replacement is recommended to contribute towards a circular economy (i.e., reduce landfills of tire waste).
4. The correlation matrix showed a strong positive correlation between compressive and tensile strength, and compressive and flexural strength was observed with a correlation coefficient of 0.93. A direct relationship was also established (through linear regression) between compressive strength and other mechanical properties (i.e., tensile and flexural strengths), and two empirical equations are proposed.

5. Weaker adhesion at the interfacial transition zone of SCRC was spotted in the microstructural analysis. Bigger micro-clusters were also observed with some deep voids, which explains the reduced hardened properties of SCRC.
6. Overall, SCRC shows poor performance under acidic attack in the durability tests. A significant reduction in compressive strength and weight loss was observed for mixes with increased PWRT, while the weight loss is more pronounced for HCL.
7. Ridge regression for compressive strength and random forest regression for tensile and flexural strength predictions were determined as the best-performing models.

FUNDING

No funding was received for the study.

COMPLIANCE WITH ETHICAL STANDARDS

This page excludes any studies that used human or animal supporters.

DECLARATION OF COMPETING INTEREST

The writers explicitly acknowledge that this manuscript is free from any competing influences and financial matters.

ACKNOWLEDGEMENT

The authors gratefully appreciate Covenant University for using their laboratory and equipment.

REFERENCES

[1] Ofuyatan, O. M., Adeniyi, A. G., Ijie, D., Ighalo, J. O., & Oluwafemi, J. (2020). Development of high-performance self-compacting concrete using eggshell powder and blast furnace slag as partial cement replacement. Construction and Building Materials, 256, 119403.

[2] Al-Osta, M. A., Ahmad, S., Al-Madani, M. K., Khalid, H. R., Al-Huri, M., & Al-Fakih, A. (2022). Performance of bond strength between ultra-high-performance concrete and concrete substrates (concrete screed and self-compacted concrete): An experimental study. Journal of Building Engineering, 51, 104291.

[3] Pang, L., Liu, Z., Wang, D., & An, M. (2022). Review on the application of supplementary cementitious materials in self-compacting concrete. Crystals, 12(2), 180.

[4] Bignozzi, M. C., & Sandrolini, F. (2006). Tyre rubber waste recycling in self-compacting concrete. Cement and concrete research, 36(4), 735-739.

[5] Yung, W. H., Yung, L. C., & Hua, L. H. (2013). A study of the durability properties of waste tire rubber applied to self-compacting concrete. Construction and Building Materials, 41, 665-672.

[6] Revilla-Cuesta, V., Skaf, M., Faleschini, F., Manso, J. M., & Ortega-López, V. (2020). Self-compacting concrete manufactured with recycled concrete aggregate: An overview. Journal of Cleaner Production, 262, 121362.

[7] Sun, C., Chen, Q., Xiao, J., & Liu, W. (2020). Utilization of waste concrete recycling materials in self-compacting concrete. Resources, Conservation and Recycling, 161, 104930.

[8] Muhit, I. B., Ahmed, S. S., Zaman, M. F., & Ullah, M. S. (2018). Effects of Multiple Supplementary Cementitious Materials on Workability and Strength of Lightweight Aggregate Concrete. Jordan Journal of Civil Engineering, 12(1), 109-124.

[9] Bilodeau, A., & Malhotra, V. M. (2000). High-volume fly ash system: concrete solution for sustainable development. Materials, 97(1), 41-48.

[10] Etli, S. (2023). Evaluation of the effect of silica fume on the fresh, mechanical and durability properties of self-compacting concrete produced by using waste rubber as fine aggregate. Journal of Cleaner Production, 384, 135590.

[11] Siddique, R. (2014). Utilization (recycling) of iron and steel industry byproduct (GGBS) in concrete: strength and durability properties. Journal of Material Cycles and Waste Management, 16, 460-467.

[12] Oluwafemi, J., Ofuyatan, O., Adedeji, A., Bankole, D., & Justin, L. (2023). Reliability assessment of ground granulated blast furnace slag/cow bone ash-based geopolymer concrete. Journal of Building Engineering, 64, 105620.

[13] Ofuyatan, O. M., Olutoge, F., Omole, D., & Babafemi, A. (2021). Influence of palm ash on properties of light weight self-compacting concrete. Cleaner Engineering and Technology, 4, 100233.

[14] Mohajerani, A., Burnett, L., Smith, J. V., Markovski, S., Rodwell, G., Rahman, M. T., ... & Maghool, F. (2020). Recycling waste rubber tyres in construction materials and associated environmental considerations: A review. Resources, Conservation and Recycling, 155, 104679.

[15] Mhaya, A. M., Huseien, G. F., Abidin, A. R. Z., & Ismail, M. (2020). Long-term mechanical and durable properties of waste tires rubber crumbs replaced GBFS modified concretes. Construction and Building Materials, 256, 119505.

[16] Roychand, R., Gravina, R. J., Zhuge, Y., Ma, X., Mills, J. E., & Youssf, O. (2021). Practical rubber pre-treatment approch for concrete use—an experimental study. Journal of Composites Science, 5(6), 143.

[17] Jiang, Y., & Zhang, S. (2022). Experimental and analytical study on the mechanical properties of rubberized self-compacting concrete. Construction and Building Materials, 329, 127177.

[18] Hilal, N. N. (2017). Hardened properties of self-compacting concrete with different crumb rubber size and content. International Journal of Sustainable Built Environment, 6(1), 191-206.

[19] Hesami, S., Hikouei, I. S., & Emadi, S. A. A. (2016). Mechanical behavior of self-compacting concrete pavements incorporating recycled tire rubber crumb and reinforced with polypropylene fiber. Journal of cleaner production, 133, 228-234.

[20] Rahman, M. M., Usman, M., & Al-Ghalib, A. A. (2012). Fundamental properties of rubber modified self-compacting concrete (RMSCC). Construction and Building Materials, 36, 630-637.

[21] Werdine, D., Oliver, G. A., de Almeida, F. A., de Lourdes Noronha, M., & Gomes, G. F. (2021). Analysis of the properties of the self-compacting concrete mixed with tire rubber waste based on design of experiments. Structures, 33, 3461-3474.

[22] Uche, O. A., Kelechi, S. E., Adamu, M., Ibrahim, Y. E., Alanazi, H., & Okokpujie, I. P. (2022). Modelling and Optimizing the Durability Performance of Self Consolidating Concrete Incorporating Crumb Rubber and Calcium Carbide Residue Using Response Surface Methodology. Buildings, 12(4), 398.

[23] Youssf, O., Swilam, A., & Tahwia, A. M. (2023). Performance of crumb rubber concrete made with high contents of heat pre-treated rubber and magnetized water. Journal of Materials Research and Technology, 23, 2160-2176.

[24] Liu, Z., Chen, X., Wang, X., & Diao, H. (2022). Investigation on the dynamic compressive behavior of waste tires rubber-modified self-compacting concrete under multiple impacts loading. Journal of Cleaner Production, 336, 130289.

[25] Li, X., Ma, F., Chen, X., Hu, J., & Wang, J. (2023). Fracture behavior investigation of self-compacting rubberized concrete by DIC and mesoscale modeling. Journal of Cleaner Production, 384, 135503.

[26] Chen, J., Zhuang, J., Shen, S., & Dong, S. (2022). Experimental investigation on the impact resistance of rubber self-compacting concrete. Structures, 39, 691-704.

[27] Feng, D. C., Liu, Z. T., Wang, X. D., Chen, Y., Chang, J.Q., Wei, D. F., & Jiang, Z. M. (2020). Machine learning-based compressive strength prediction for concrete: An adaptive boosting approach. Construction and Building Materials, 230, 117000.

[28] Gholampour, A., Gandomi, A., & Ozbakkaloglu, T. (2017). New formulations for mechanical properties of recycled aggregate concrete using gene expression programming. Construction and Building Materials, 130, 122–145.

[29] Azizifar, V. & Babajanzadeh, M. (2018). Compressive Strength Prediction of Self-Compacting Concrete Incorporating Silica Fume Using Artificial Intelligence Methods. Civil Engineering Journal. 4 (7).

[30] Serraye, M., Kenai, S., & Boukhatem, B. (2021). Prediction of compressive strength of self-compacting concrete (SCC) with silica fume using neural networks models. Civil Engineering Journal, 7(1), 118-139.

[31] Kaloop, M. R., Kumar, D., Samui, P., Hu, J. W., & Kim, D. (2020). Compressive strength prediction of high-performance concrete using gradient tree boosting machine. Construction and Building Materials, 264, 120198.

[32] de-Prado-Gil, J., Palencia, C., Silva-Monteiro, N., & Martínez-García, R. (2022). To predict the compressive strength of self compacting concrete with recycled aggregates utilizing ensemble machine learning models. Case Studies in Construction Materials, 16, e01046.

[33] Li, P., Khan, M. A., El-Zahar, E. R., Awan, H. H., Zafar, A., Javed, M. F., ... & Wang, F. (2022). Sustainable use of chemically modified tyre rubber in concrete: Machine learning based novel predictive model. Chemical Physics Letters, 139478.

[34] Topcu, I. B., & Sarıdemir, M. (2008). Prediction of rubberized concrete properties using artificial neural network and fuzzy logic. Construction and Building Materials, 22, 532–540.

[35] Gesoglu, M., Guneyisi, E., Ozturan, T., & Ozbay, E. (2010). Modeling the mechanical properties of rubberized concretes by neural network and genetic programming. Materials and Structures, 43, 31-45.

[36] Sun, Y., Li, G., Zhang, J., & Qian, D. (2019). Prediction of the strength of rubberized concrete by an evolved random forest model. Advances in Civil Engineering, 2019, 5198583.

[37] Hadzima-Nyarko, M., Nyarko, E. K., Lu, H., & Zhu, S. (2020). Machine learning approaches for estimation of compressive strength of concrete. The European Physical Journal Plus, 135, 682.

[38] Gregori, A., Castoro, C., & Venkiteela, G. (2021) Predicting the compressive strength of rubberized concrete using artificial intelligence methods. Sustainability, 13, 7729.

[39] Huang, X., Zhang, J., Sresakoolchai, J., & Kaewunruen, S. (2021). Machine learning aided design and prediction of environmentally friendly rubberized concrete. Sustainability, 13, 1691.

[40] Zhang, J., Ma, G., Huang, Y., Aslani, F., & Nener, B. (2019). Modelling uniaxial compressive strength of lightweight self-compacting concrete using random forest regression. Construction and Building Materials, 210, 713-719.

[41] Kovačević, M., Lozančić, S., Nyarko, E. K., & Hadzima-Nyarko, M. (2021). Modeling of compressive strength of self-compacting rubberized concrete using machine learning. Materials, 14(15), 4346.

[42] Ighalo, J. O., & Adeniyi, A. G. (2020). A Perspective on Environmental Sustainability in the Cement Industry. Waste Disposal and Sustainable Energy, 2, 161-164.

[43] United Nations (2015). The UN Sustainable Development Goals. Available from https://sdgs.un.org/goals (accessed on 20/04/2023).

[44] HM Government. (2022). The Construction Playbook: Government Guidance on sourcing and contracting public works projects and programmes. Version 1.1, The Cabinet office, His Majesty's Government, The United Kingdom.

[45] Muhit, I. B. (2013). Dosage Limit Determination of Superplasticizing Admixture and Effect Evaluation on Properties of Concrete. International Journal of Scientific and Engineering Research, 4(3).

[46] Olowofoyeku A, M., Ofuyatan O. M., Oluwafemi J., Ajao O., David O., Effect of Superplasticizer on Workability and Properties of Self-Compacting Concrete Journal of Physics: Conference Series, 1378 (4).

[47] Hameed, A. H. (2012). Effect of superplasticizer dosage on the workability of self compacting concrete. Diyala Journal of Engineering Sciences, 5(2), 66-81.

[48] Sua-iam, G. & Makul, N. (2014). Utilization of high volumes of unprocessed lignite-coal fly ash and rice husk ash in self-consolidating concrete. Journal of Cleaner Production, 78, 184-194.

[49] Meko B., Ighalo J., Ofuyatan O., Enhancement of self-compactability of fresh self-compacting concrete: A review. Cleaner Materials, 1(2021), 100019.

[50] Madandoust, R. & Mousavi, S. Y. (2012). Fresh and hardened properties of self-compacting concrete containing metakaolin. Construction and Building Materials, 35, 752-760.

[51] Ofuyatan O. M., Omole D., Kayode-Thomas E., Ogundeji O., (2022) Marble waste and recycled concrete aggregates in self compacting concrete (SSC): an evaluation of fresh and hardened properties, Australian Journal of Civil Engineering, 20(1), 67-79

[52] BS EN 206. (2013). Concrete – Specification, performance, production and conformity, British Standards Institution, London.

[53] ASTM Standard C496-96. (2017). Standard Test Method for Splitting Tensile Strength of Cylindrical Concrete Specimens. ASTM International, West Conshohocken, PA. DOI: 10.1520/C0496-96.

[54] ASTM Standard C78 (2022). Standard Test Method for Flexural Strength of Concrete (Using Simple Beam with Third-Point Loading). ASTM International, West Conshohocken, PA. DOI: DOI: 10.1520/C0078_C0078M-22

[55] Steyn, Z. C., Babafemi, A. J., Fataar, H., & Combrinck, R. (2021). Concrete containing waste recycled glass, plastic and rubber as sand replacement. Construction and Building Materials, 269, 121242.

[56] Flores-Medina, D., Flores Medina, N., & Hernández-Olivares, F. (2014). Static mechanical properties of waste rests of recycled rubber and high quality recycled rubber from crumbed tyres used as aggregate in dry consistency concretes. Materials and structures, 47, 1185-1193.

[57] Ling, T. C. (2011). Prediction of density and compressive strength for rubberized concrete blocks. Construction and Building Materials, 25(11), 4303-4306.

[58] Ofuyatan, O. M., Agbawhe, O. B., Omole, D. O., Igwegbe, C. A., & Ighalo, J. O. (2022). RSM and ANN modelling of the mechanical properties of self-compacting concrete with silica fume and plastic waste as partial constituent replacement. Cleaner Materials, 4, 100065.

[59] Adeboje, A. O., Kupolati, W. K., Sadiku, E. R., Ndambuki, J. M., & Kambole, C. (2020). Experimental investigation of modified bentonite clay-crumb rubber concrete. Construction and Building Materials, 233, 117187.

[60] Raffoul, S., Garcia, R., Pilakoutas, K., Guadagnini, M., & Medina, N. F. (2016). Optimization of rubberized concrete with high rubber content: An experimental investigation. Construction and Building Materials, 124, 391-404.

[61] Dhiyaneshwaran S., Ramanathan P., Baskar I., & Venkatasubramani R. (2013). Study on durability characteristics of self-compacting concrete with fly ash. Jordan Journal of Civil Engineering, 7, 342–352.

[62] Ofuyatan, O. M., Olutoge, F. A., & Olowofoyeku, O. A. (2015). Durability properties of palm oil fuel ash self- compacting concrete. Engineering, Technology & Applied Science Research, 5(1), 753-756.

[63] Graw, M. (2018). Putting Supervised and Unsupervised Learning to Work for Your Business.

https://medium.com/@michaelgraw/putting-supervised-and-unsupervised-learning-to-work-for-your-business-c7bb68f50efa (accessed on 20/04/2023).

[64] Shapiro, S. S., & Wilk, M. B. (1965). An analysis of variance test for normality (complete samples). Biometrika, 52 (3 - 4), 591–611.